

## Stable violet cathodoluminescence of $\alpha$ -quartz after Ge + implantation at elevated temperature

P. K. Sahoo, S. Dhar, S. Gasiorek, and K. P. Lieb

Citation: *Journal of Applied Physics* **96**, 1392 (2004); doi: 10.1063/1.1767973

View online: <http://dx.doi.org/10.1063/1.1767973>

View Table of Contents: <http://scitation.aip.org/content/aip/journal/jap/96/3?ver=pdfcov>

Published by the [AIP Publishing](#)

---

### Articles you may be interested in

[Light-emitting defects and epitaxy in alkali-ion-implanted  \$\alpha\$  quartz](#)

*Appl. Phys. Lett.* **88**, 261102 (2006); 10.1063/1.2215615

[Achieving epitaxy and intense luminescence in Ge/Rb-implanted  \$\alpha\$ -quartz](#)

*Appl. Phys. Lett.* **87**, 021105 (2005); 10.1063/1.1994953

[Cathodoluminescence and solid phase epitaxy in Ba-irradiated  \$\alpha\$ -quartz](#)

*J. Appl. Phys.* **97**, 014910 (2005); 10.1063/1.1829791

[Cathodoluminescence versus dynamical epitaxy of Ba-ion irradiated  \$\alpha\$ -quartz](#)

*Appl. Phys. Lett.* **85**, 1341 (2004); 10.1063/1.1784538

[Chemically guided epitaxy of Rb-irradiated  \$\alpha\$ -quartz](#)

*J. Appl. Phys.* **95**, 4705 (2004); 10.1063/1.1689733

---



# Stable violet cathodoluminescence of $\alpha$ -quartz after Ge<sup>+</sup> implantation at elevated temperature

P. K. Sahoo,<sup>a)</sup> S. Dhar,<sup>b)</sup> S. Gasiorek, and K. P. Lieb

*II. Physikalisches Institut, Universität Göttingen, Tammannstrasse 1, D-37077 Göttingen, Germany*

(Received 2 December 2003; accepted 11 May 2004)

Doping single-crystalline  $\alpha$ -quartz with 120 keV Ge<sup>+</sup>-ion implantation under the conditions of dynamic solid phase epitaxial regrowth has been studied as function of ion fluence and substrate temperature. In particular, the light emitting properties possibly suitable for optoelectronic devices have been investigated by measuring cathodoluminescence spectra for implantation temperatures from 300 to 1223 K and for analyzing temperatures from 10–300 K. Rutherford backscattering channeling analysis showed that the Ge implantation produced amorphous layers varying in depth with temperature. At a fluence of  $7 \times 10^{14}$  Ge-ions/cm<sup>2</sup> and an implantation temperature of 1073 K, Ge implantation is accompanied by a strong increase in the luminescence intensity of a violet band, which we associate with Ge-related defects or Ge clusters. This violet band is very stable and has a long lifetime of 6  $\mu$ s. All the other bands observed are connected to known oxygen defect centers in the SiO<sub>2</sub> network. © 2004 American Institute of Physics. [DOI: 10.1063/1.1767973]

## I. INTRODUCTION

A promising approach of designing Si-based light-emitting materials is the ion implantation of luminescent species into thin amorphous SiO<sub>2</sub> (a-SiO<sub>2</sub>) films, thermally grown on Si substrates. Likewise, considerable effort has been made to develop ion-implanted synthetic  $\alpha$ -quartz for fabricating various optoelectronic and photonic devices such as optical insulators, waveguides, and switches.<sup>1–5</sup> In the last two decades, many investigations have been devoted to doping a-SiO<sub>2</sub> with metal, semiconductor, or rare-earth element ions, using various processing techniques. For example, strong luminescence in the visible range (violet and blue bands) was observed after Ge or Si ion implantation into a-SiO<sub>2</sub> followed by high-temperature postimplantation annealing.<sup>6,7</sup> The intensity and spectral shape of the luminescent light indeed sensitively depend on the implantation and annealing conditions, but the thermal and chemical surroundings during growth are not well under control. As an alternative, modifying the optical properties of single-crystalline synthetic  $\alpha$ -quartz by ion implantation is a dry process, and thus possibly more advantageous, although quartz easily becomes amorphous during ion implantation.<sup>8,9</sup> Hence, simultaneously achieving a higher light emission by appropriate doping and better epitaxial recovery of quartz is a challenge. Optimized processing parameters such as ion species, fluence and energy, and substrate temperature have to be tuned in order to test the feasibility of the method in applications.

In recent years, two processes have been developed to achieve solid phase epitaxial regrowth (SPEG) of ion-damaged  $\alpha$ -quartz. In dynamic epitaxy, the ions are implanted into the quartz sample at elevated temperatures in such a fashion that the formation of defects is counterbal-

anced by the thermal recrystallization process.<sup>10</sup> In chemically guided epitaxy, alkali-ion implantation followed by thermal annealing in air or oxygen leads to full or partial epitaxy of the a-SiO<sub>2</sub> layers.<sup>11</sup> Based on our recent results concerning the generation of cathodoluminescence (CL) after Ba implantation and dynamic annealing in quartz,<sup>12</sup> we report here on the measurements of CL light in  $\alpha$ -quartz emitted after Ge-ion irradiation at elevated sample temperatures, without fully destroying its single-crystalline structure. To this end, the influence of several processing parameters, such as ion energy, fluence and flux, and sample and CL temperature, was studied.

Due to its higher spatial resolution and optical penetration depth, keV-electron-induced CL spectroscopy<sup>13–15</sup> provides mainly information about the defects in SiO<sub>2</sub> layers. Information on the stability and lifetime mechanism of different luminescence bands can be gained by means of time-resolved CL spectroscopy. The present work is devoted to maximizing the CL light output and minimizing the defect production in quartz during Ge-ion implantation. The optimal fluence of  $7 \times 10^{14}$  Ge-ions/cm<sup>2</sup> has been fixed from our previous study.<sup>16</sup> The present CL study has also been performed to identify the defect centers associated with different visible emission bands. A violet band corresponding to the implanted Ge in the SiO<sub>2</sub> matrix was found to be the most dominant one, reaching its maximum intensity at about  $7 \times 10^{14}$  Ge-ions/cm<sup>2</sup> and 1073 K sample temperature.

## II. EXPERIMENTS

Well polished samples of synthetic  $\alpha$ -quartz, (0001) oriented and  $10 \times 10$  mm<sup>2</sup> in size, were irradiated with 120 keV Ge<sup>+</sup> ions at temperatures ranging from 300 K to 1223 K and for fluences up to  $1 \times 10^{16}$  ions/cm<sup>2</sup>; as mentioned before, the optimized fluence was  $7 \times 10^{14}$  Ge-ions/cm<sup>2</sup>. The samples were mounted on a copper target holder, connected to a ceramic heater and equipped with a thermocouple. The ion flux density was kept constant at all

<sup>a)</sup>On leave from Department of Physics, Indian Institute of Technology, Kanpur 208016, India.

<sup>b)</sup>Present address: Physics Department, University of Maryland, College Station, Maryland 20742.

the temperatures. Homogeneous implantations with a beam current of  $0.5 \mu\text{A}$  were performed over half the sample area using a *xy*-electrostatic scanner. The beam flux was  $3 \times 10^{12}$  ions/cm<sup>2</sup> s for all the samples. The projected range  $R_p$  obtained from a SRIM simulation<sup>17</sup> was about 69 nm. During each implantation, the other half of the sample surface was covered with an Al foil in order to preserve an unmodified area required for sample orientation during the channeling analysis. The damage analysis and Ge depth distribution were monitored by means of Rutherford backscattering channeling spectroscopy (RBS-C) with a 0.9 MeV He<sup>++</sup> beam using a Si surface barrier detector of 12 keV resolutions, positioned at 165° to the beam direction. All the implantations and RBS-C analyses were performed using the Göttingen 500 kV ion implanter IONAS.<sup>18</sup> The Ge depth profiles were deduced with the RUMP code<sup>19</sup> and the apparent damage distributions of the SiO<sub>2</sub> matrix with the DAMAGE code.<sup>20</sup>

After Ge implantation cathodoluminescence spectra were recorded in the temperature range of 10–300 K. The samples were mounted on an oxygen free copper target head of a closed cycle helium cryostat and irradiated with a 5 keV electron beam of 1 W/cm<sup>2</sup> power density (Specs EQ-22). The CL light was collected using an achromate lens and monitored by means of a photomultiplier tube (Hamamatsu R928) after focusing into a Czern-Turn spectrograph (Jobin Yvon 1000M). Each CL spectrum was collected for a total time of 700 s, taking 1 nm/s steps in the wavelength range of 200–900 nm with a 1200 lines/mm grating. The deconvolution of the CL spectra was done with up to five Gaussian-shaped subbands after conversion to the energy scale as described in Ref. 13. The CL emission intensities of all the subbands were corrected for the instrument response function, which was determined using a standard halogen calibration lamp. Time-resolved CL measurements were performed with a pulsed electron beam using a constant fraction discriminator (Ortec-473 A) and a multichannel scalar (Fast COM 7882). The CL measurements were repeated on different spots in order to check the data reproducibility. We noted that even long electron irradiations did not change the shape and position of these peaks, except for slight variations in the intensities.

### III. RESULTS AND DISCUSSION

#### A. Dynamic solid phase epitaxy

Figure 1(a) shows the RBS-channeling spectra taken after Ge-ion implantation as a function of the irradiation temperature. For comparison, a random and channeling (virgin) spectrum of a nonirradiated sample are also shown. For nonirradiated samples, the minimum channeling yield  $\chi_{\min}=5\%$  in the virgin  $\alpha$ -quartz indicates the good crystal quality. After Ge implantation at RT and at a fluence  $7 \times 10^{14}$  ions/cm<sup>2</sup> (critical fluence for maximum light emission), the height of the RBS signals from both the Si and O sublattice in the near-surface region reach the random level suggesting the formation of a homogeneous amorphous layer of about 160 nm thickness. For increasing sample temperature, the thickness of this amorphous layer decreases, indicating a planar recrystallization process during dynamic epitaxy. We

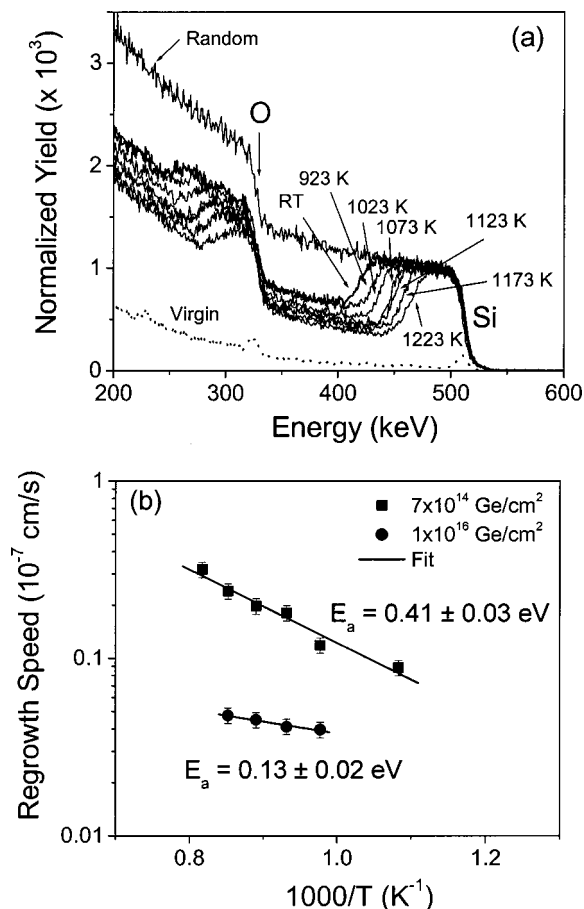


FIG. 1. (a) RBS-channeling spectra display partial dynamic SPEG of quartz after 120 keV Ge<sup>+</sup> ion implantation to a fluence of  $7 \times 10^{14}$  ions/cm<sup>2</sup>. Also shown are the channeling and random spectra of a nonirradiated sample (virgin conditions). (b) Regrowth speed of Ge-doped quartz as a function of sample temperature.

failed to reach complete recrystallization even at the highest sample temperature of 1223 K in vacuum. The Ge profiles in all the cases were almost Gaussian shaped; the measured average projected range of 65 nm compares rather well with the value of 69 nm calculated with the program SRIM.<sup>17</sup> The Ge implantation profile at 1173 K and above a fluence of  $1 \times 10^{15}$  ions/cm<sup>2</sup> has a bimodal Gaussian shape;<sup>16,21</sup> it also depends on the irradiation temperature. It may be noted that no SPEG occurred after Ge implantation at RT followed by vacuum annealing at 1173 K for 1 h.

From the damage profile, the regrowth speed of the epitaxially recovered layer was determined and is plotted in Fig. 1(b) as a function of temperature. It follows an Arrhenius dependence with an activation energy of  $E_a=0.41 \pm 0.03$  eV (at  $\Phi=7 \times 10^{14}$  ions/cm<sup>2</sup>). This value is much higher than the one obtained for 50 keV Ne ions [0.26 eV (Ref. 11)] or 175 keV Ba ions [0.24 eV (Ref. 10)] implanted into quartz. This suggests that the defect annihilation mechanism during dynamic annealing in the case of photoactive ions such as Ge may differ from the one for Ba and Ne ions. At the higher fluence of  $1 \times 10^{16}$  ions/cm<sup>2</sup>, the activation energy was reduced to  $E_a=0.13 \pm 0.02$  eV. At this fluence the recovery due to dynamic annealing is very small. Our results also suggest that the activation energy strongly depends on the ion fluence

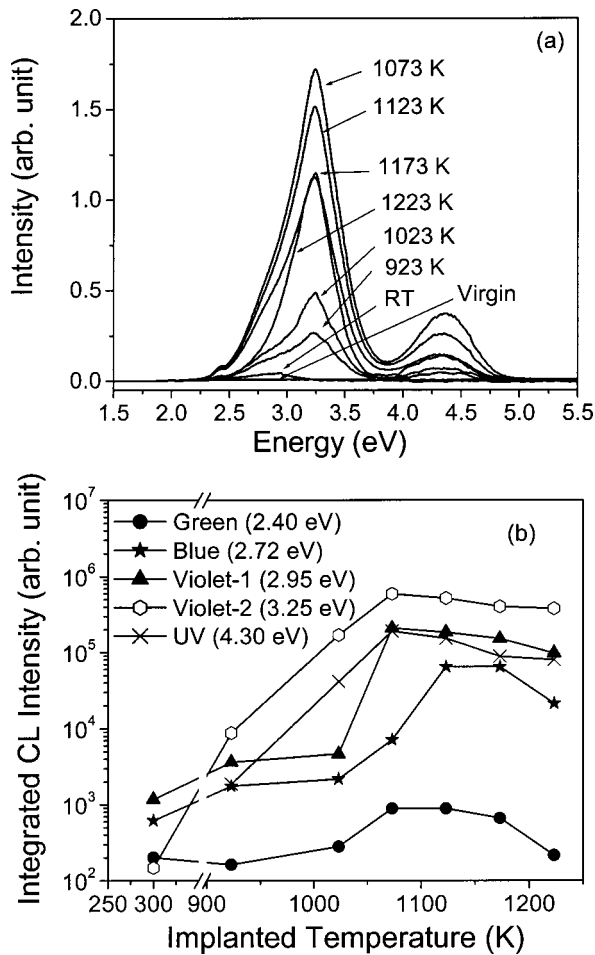


FIG. 2. (a) Cathodoluminescence spectra taken at RT for Ge-irradiated  $\alpha$ -quartz; the implantation temperature varied between 300 and 1223 K; (b) temperature dependence of the integrated intensities of the subpeaks.

and flux. The fluence-dependent dynamic annealing<sup>16</sup> shows that the amorphization saturates above a critical Ge-ion fluence of  $5 \times 10^{14}$  ions/cm<sup>2</sup>.

### B. Cathodoluminescence spectra taken at 300 K

Figure 2(a) illustrates the CL spectra taken at room temperature before and after Ge-implantation at various sample temperatures. The average energies and full width at half maximum (FWHM) of the resolved CL emission bands and their interpretations are summarized in Table I and will be discussed below. The uncertainties of the numbers given indicate the maximum deviations from the mean positions and mean FWHM determined in the fits. When the spectra were fitted with two emission bands at 2.95 and 3.25 eV, their

FWHM and peak positions remained constant, while combining these two bands into a single one located at 3.1 eV introduced larger fluctuations of its FWHM and integrated intensity.

The intensities of the Gaussian-shaped subpeaks corresponding to the different emission bands are plotted in Fig. 2(b) as a function of the implantation temperature. The virgin sample displays a broad peak at 2.72 eV and a narrow peak at 2.40 eV with very weak intensities, corresponding to blue and green bands, respectively. The energy of the 2.72 eV band agrees with that of the previously observed blue band,<sup>22,23</sup> which however slightly varies with the quality and impurity concentration<sup>13</sup> of the quartz samples. The weak 2.40 eV band has been previously observed by Fitting *et al.*<sup>22,23</sup> and by Stevens-Kalceff and Philips,<sup>13</sup> but with a larger width and slightly different energies. According to Refs. 14 and 21–24, green and blue bands associated precursors in SiO<sub>2</sub> generated by the electron-beam irradiation. The UV bands were detected at room temperature, whereas cooling the crystal to 10 K lead to the appearance of a blue band at 2.72 eV with a strong increase of the broadly structured band. This peak appeared after lowering the analyzing temperature to 200 K and reached its maximum at 100 K.

After the implantation of  $7 \times 10^{14}$  Ge<sup>+</sup>-ions/cm<sup>2</sup> at 923–1223 K, the room-temperature CL spectra showed five bands at 511 nm (2.40 eV, green=G), 455 nm (2.72 eV, blue=B), 420 nm (2.95 eV, violet-1=V1), 382 nm (3.25 eV, violet-2=V2), and 288 nm (4.30 eV, UV). Their intensities increase with increasing implantation temperature, reach maximum values at 1073 K and finally saturate at somewhat lower values. Except for the violet band, all the other bands were associated with various known defect centers in the SiO<sub>2</sub> matrix, created either by ion implantation or by electron irradiation during the CL measurements. The blue and UV bands are connected to oxygen-deficient centers (ODC,  $\equiv$ Si-Si $\equiv$ ).<sup>14,22</sup> The green peak at 2.40 eV may be connected to oxygen vacancy interstitial pairs [V<sub>o</sub>; (O<sub>2</sub>)], where V<sub>o</sub> denotes an oxygen vacancy,<sup>25</sup> or to radiation-induced self-trapped excitons within the top a-SiO<sub>2</sub> layer containing a large number of peroxy linkages (Si-O-O-Si).<sup>14,26</sup> The intensity variation of the green band is similar to that of the blue band.

The dominant violet singlet-singlet luminescence band at 3.25 eV is unambiguously related to the implanted species Ge and obviously not related to precursors or electron-irradiation defects of the SiO<sub>2</sub> matrix.<sup>22,25–28</sup> The top amorphous SiO<sub>2</sub> layer containing no implanted impurity ions leads to only blue, green, and red luminescence. But the

TABLE I. The mean CL emission bands observed at RT after Ge-ion irradiations in  $\alpha$ -quartz at 300–1223 K.

Energy (eV)	Wavelength (nm)	FWHM (eV)	Identification
2.40±0.02	511, Green	0.16±0.02	Oxygen vacancy interstitial pairs
2.72±0.01	455, Blue	0.31±0.03	E' center, ODC center
2.95±0.02	420, Violet-1	0.34±0.02	Ge related defect center (Si-Ge/Ge-Ge)
3.25±0.02	382, Violet-2	0.33±0.02	Ge related defect center (Si-Ge/Ge-Ge)
4.30±0.02	288, UV	0.29±0.03	ODC center

small amount of implanted Ge in SiO<sub>2</sub> generates the intense violet band and thus is most probably related to Ge-associated defects. When the irradiation temperature was increased from 1073 to 1223 K, the intensity ratio of blue to violet band decreased. At 1223 K, the blue band was almost absent and the peak could be fitted with only the violet component.

It may be noted that the CL spectra show two closely spaced violet subbands at 2.95 and 3.25 eV, in Fig. 2(b). According to Kim *et al.*,<sup>29</sup> implantation of Ge produces the GeO<sub>2</sub> and metastable GeO oxide phases in SiO<sub>2</sub>, after vacuum annealing the Ge-irradiated  $\alpha$ -SiO<sub>2</sub> samples. But the x-ray photoelectron spectroscopy results of these authors also showed that the Ge-Ge bonds were relatively more often formed than the Ge-O bonds, which are the origin of the luminescence bands in the SiO<sub>2</sub> layer. Fitting *et al.*<sup>21,22</sup> reported that the violet band at 3.1 eV is due to the Ge dopant centers in rutile coordination and the intensity of this violet band increases strongly after annealing. In our line of interpretation, an oxygen atom is removed from the SiO<sub>2</sub> network in the process of either Ge doping at high temperatures or postannealing after Ge or Si implantation; the Si-Si bond forms<sup>29</sup> and extends to Si-Ge and Ge-Ge bonds. It is also known that the E' center<sup>30</sup> produced during Ge implantation into thin SiO<sub>2</sub> films transform the Si-Ge and Ge-Ge centers; at higher temperature Ge-nanoclusters forms. We assume a similar effect for the formation of Ge-related centers, which are the origin of the violet band. Very weak violet bands were observed after Ge implantation at room temperature, whose intensity increased by four orders of magnitude after implantation at 1073 K. We infer that three types of defect centers (Si-Ge, Ge-Ge, and Ge nanoclusters) are responsible for the violet band at 2.95 eV and 3.25 eV produced during Ge implantation at elevated temperature. The intensities of these violet subbands depend on the implantation temperature and this indicates that the abundance of the various defects varies with temperature. The formation of nanoclusters after Ge implantation into  $\alpha$ -quartz at high temperatures has also been reported by the Rossendorf group.<sup>7,30,31</sup>

### C. Temperature dependence of CL

This part of the experiments aimed at optimizing the CL light output as function of the sample temperature  $T_{CL}$  during electron bombardment, by using ion irradiation conditions close to those for (partial) epitaxy, i.e. a Ge fluence around  $7 \times 10^{14}$  Ge-ions/cm<sup>2</sup> and implantation temperatures of 1073 and 1173 K. In Fig. 3, the intensity of the violet band as function of the CL temperature  $T_{CL}$  and for the different implantation conditions is displayed. Above  $T_{CL} = 200$  K, the violet band is stable in all the cases, but reaches maximum intensity between  $T_{CL} \approx 100-150$  K. At higher fluences the violet band has almost constant intensity. We tend to conclude again that both the irradiation temperature and ion fluence are responsible for forming the Ge-related ODC centers for violet luminescence. As it is well known in CL work, the usually strong temperature dependence of non-radiative transitions does not allow a more refined analysis of these data.

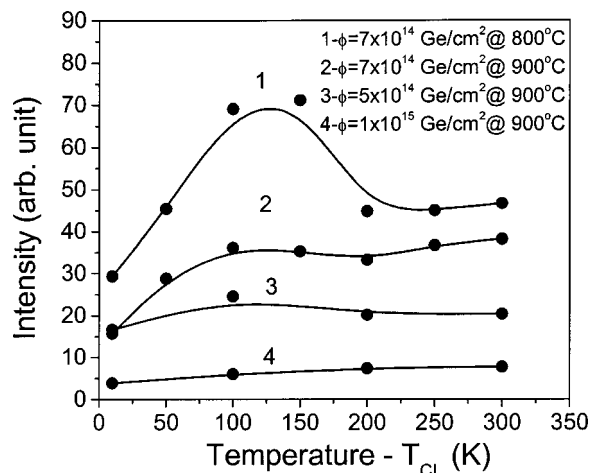


FIG. 3. Integrated intensity of the violet band after Ge irradiation at 1073 and 1173 K and for fluences of  $7 \times 10^{14}$  to  $1 \times 10^{15}$  Ge-ions/cm<sup>2</sup> plotted vs the CL temperature  $T_{CL}$ .

Finally, the CL spectra were measured as a function of the sample temperature  $T_{CL}$  after Ge-ion implantation at 1073 K with a fluence of  $7 \times 10^{14}$ /cm<sup>2</sup> (optimized CL output). As seen from Fig. 4(a), the blue peak is dominant at 10 K, while the violet peak is dominant at 300 K and stable up to 200 K. The intensity variations of both peaks as a function of the CL temperature are shown in Fig. 4(b). The

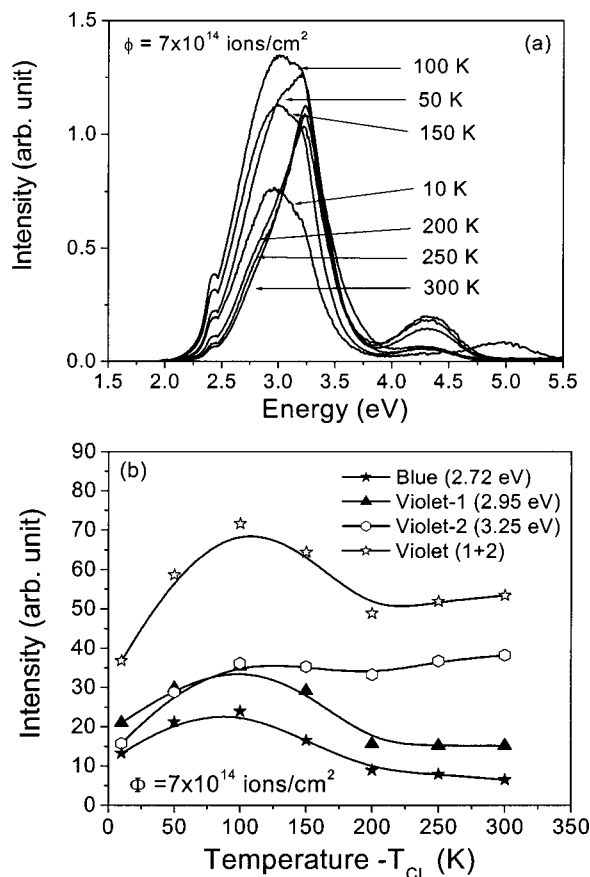


FIG. 4. (a) Temperature-dependent CL spectra taken for samples irradiated at 1073 K with the optimized fluence of  $7 \times 10^{14}$  Ge-ions/cm<sup>2</sup>. (b) Integrated intensities for the blue and violet bands as a function of CL temperature  $T_{CL}$ .

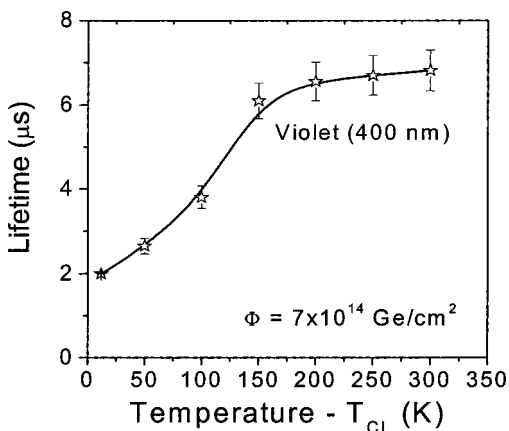


FIG. 5. The lifetime  $\tau$  of the decay curve of the violet band (400 nm) measured as function of the CL temperature  $T_{CL}$ .

two violet subbands and their sum are clearly observed. Above 100 K, the 2.95 eV (violet-1) band decreases in intensity whereas the 3.25 eV (violet-2) increases monotonically. This suggests that the lifetime of the violet band, which originates from Ge defects in the  $SiO_2$  network, also changes with temperature, due to the temperature dependence of the oxygen mobility during implantation. The lifetime of this violet band has been extracted by exponential fitting the time-resolved CL decay curve and is shown in Fig. 5. Below 150 K, this lifetime increases linearly and above 150 K it has an almost constant value of  $\tau=6 \mu s$ . According to Skuja,<sup>26,32</sup> the Ge-related ODC centers have luminescence lifetimes of  $\approx 110 \mu s$  for the  $T_1 \rightarrow S_0$  transition and 5.5–6.5 ns for the  $S_1 \rightarrow S_0$  emission. In the present experiment we attribute the observed lifetimes of 2.0–7.2  $\mu s$  to the singlet-singlet transition in Ge-related ODC centers after Ge irradiation of  $\alpha$ -quartz at high temperature. In contrast to achieving as complete as possible dynamic epitaxy at the highest sample temperature, we optimized here the implantation parameters to achieve the highest CL output. For increasing implantation temperature the Ge-related defect centers are distributed in such a fashion as to produce a high violet luminescence at 1073 K. We interpret this finding as the formation of Ge-Ge and Si-Ge defect centers uniformly spread over the volume and giving rise to violet luminescence. Above 1073 K the Ge-related defects coagulate and their average volume and luminescence yield decrease. On the other hand the CL intensity reaches a maximum at around 150 K and remains stable up to 300 K in the temperature dependence CL. The ratio of the violet to blue band becomes negative above 150 K.

#### D. Comparison with results obtained via room temperature implantation

Among the basic questions of PL or CL spectroscopy in quartz and silica are the origins of the various bands and their correlation with the microstructures of the color centers. Quantum confinement of the nanoparticles, molecularlike atomic arrangements of the implanted atoms within the (damaged) matrix, and its constituents and substitutional implanted atoms (with and without lattice defects) have been

discussed. At this point it may therefore be appropriate to compare our results with those recently obtained by Lopes *et al.*,<sup>33</sup> who implanted  $1.6 \times 10^{16}$  120 keV Ge-ions/cm<sup>2</sup> into a- $SiO_2$  at room temperature and annealed the samples for 30 min under  $N_2$  at 763–1173 K. Using a combination of RBS, TEM, and photoluminescence (PL), these authors correlated the PL spectra with the nanocluster size distribution as deduced from TEM and the overall Ge depth profile in a- $SiO_2$  as deduced from RBS. For increasing annealing temperature, the mean cluster size was found to increase from 2.2 nm at 673 K to 5.6 nm at 1173 K, while the standard deviation of the distribution increased from 0.5 to 1.7 nm. Simultaneously the fraction of Ge-atoms in these nanoclusters (visible in TEM and having a diameter of  $>0.8$  nm) rose from 43% (at 873 K) to 75% (at 1173 K). The PL emission spectra after 5.17 eV UV excitation showed an UV component at 4.25 eV and a blue-violet component at 3.2 eV. Parallel to the coarsening process of the Ge nanoclusters, the blue-violet PL emission intensity increased by more than an order of magnitude between 673 to 1173 K. Also the intensity of the UV component was rising.

We first note the similarity of the blue-violet band in the PL work (centered at 3.2, 0.45 eV FWHM) with the violet bands observed in the present CL study (2.95, 0.34 eV FWHM; 3.25, 0.33 eV FWHM, see Table I). Furthermore as shown in Fig. 2(a), the CL spectra taken at RT exhibit a UV component at 4.30 eV (FWHM: 0.29 eV), which lines up with a corresponding component in the PL spectra.<sup>33</sup> The intensities of both CL bands increase strongly with implantation temperature up to 1073 K and then decrease slowly [see Fig. 2(b)]. This finding is again in line with the results by Lopes *et al.*<sup>33</sup> Lacking a quantitative comparison of intensities between the two experiments, the most striking difference relates to the other components of the CL spectra shown in Figs. 2(a) and 4(a), which were not present in the PL spectra.<sup>33</sup> As to the interpretation of the PL spectra, Lopes *et al.*<sup>33</sup> pointed out that a large fraction of the implanted Ge atoms, even after ripening at 1173 K, did not form visible nanoparticles and that the PL light did not depend on the size of the nanoparticles. This finding implies that quantum confinement, which would require a redshift for progressing cluster ripening, is not the primary PL mechanism.

Meinardi and Paleari<sup>34</sup> have proposed an alternative interpretation of the peak at 3.1 eV in their synchrotron-excited PL work after neutron irradiations of Ge-doped silica and fused quartz. According to their study, this peak is in no peculiar way related to Ge itself, but rather to the radiation damage produced by ions and neutrons. It is concluded, “different arrangements of the defect environment, dependent on the different defect-formation processes, play the key role in determining the observed PL features.”

#### IV. CONCLUSIONS

Dynamic epitaxy and cathodoluminescence of  $\alpha$ -quartz after Ge<sup>+</sup>-ion irradiation at high temperature in the range of 923–1223 K and at fluences of  $7 \times 10^{14}$  and  $1 \times 10^{16}$  ions/cm<sup>2</sup> have been studied. In this temperature range, only partial epitaxy of the radiation-damaged silica

matrix was found. For the optimal fluence of  $7 \times 10^{14}$  Ge<sup>-</sup>ions/cm<sup>2</sup>, the deduced activation energy for progression of the a/c interface (0.41 eV) is higher than for  $1 \times 10^{16}$  Ge<sup>-</sup>ions/cm<sup>2</sup> (0.13 eV). At the optimized fluence of  $7 \times 10^{14}$  ions/cm<sup>2</sup> and irradiation temperature of 1073 K, several bands in the CL spectra were observed between 10 and 300 K CL temperature. The dominant violet band at 3.1 eV is tentatively associated with Ge-related defects produced during the Ge implantation at elevated temperature. It features a rather long decay constant of  $\tau=6 \mu\text{s}$  at  $T_{\text{CL}} > 150$  K, as observed from time-resolved CL spectroscopy. It is interesting to note that 120-keV Ge-ion implantation in silica at room temperature, followed by thermal annealing under N<sub>2</sub> atmosphere led to a similar violet band in the PL analysis. The light output of these Ge-related luminescence centers strongly depends on the irradiation temperature and fluence and on the CL observation temperature. Other well-known bands (blue, 2.72 eV; green, 2.40 eV; and UV, 4.30 eV) are related to different known defect centers in the SiO<sub>2</sub> matrix due to electron irradiation. Further studies are required, especially with regard to PL and TEM measurements in order to elucidate the luminescence mechanism and the local environments of the implanted species. As in our recent CL and SPEG investigations after Ba or Rb implantation in quartz,<sup>13,35</sup> experiments at elevated implantation temperatures appear useful to reach these goals.

## ACKNOWLEDGMENTS

The authors are grateful to Professors H. Hofsäss and V. N. Kulkarni, Dr. U. Vetter, Dr. M. Uhrmacher, and D. Purschke for their help and advice during some of the measurements and discussions. This work was funded by Deutsche Forschungsgemeinschaft (DFG).

<sup>1</sup>P. J. Chandler, F. L. Lama, P. D. Townsend, and L. Zhang, *Appl. Phys. Lett.* **53**, 89 (1988).

<sup>2</sup>B. G. Yacobi and D. B. Holt, *J. Appl. Phys.* **59**, R1 (1986).

<sup>3</sup>J. Albert, in *Introduction to Glass Integrated Optics*, edited by S. I. Najafi (Artech House, Boston, 1992).

<sup>4</sup>Y. J. Chabal, *Fundamental Aspects of Silicon Oxidation* (Springer, Heidelberg, 2001).

<sup>5</sup>G. Roma, Y. Limoge, and S. Baroni, *Phys. Rev. Lett.* **86**, 4564 (2001).

<sup>6</sup>J. von Borany, R. Grötzschel, K. H. Heinig, A. Markwitz, W. Matz, B. Schmidt, and W. Skorupa, *Appl. Phys. Lett.* **71**, 3215 (1997).

<sup>7</sup>L. Rebohle, J. von Borany, R. A. Yankov, W. Skorupa, I. E. Tyschenko, H. Fröb, and K. Leo, *Appl. Phys. Lett.* **77**, 969 (2000).

<sup>8</sup>F. Harbsmeier and W. Boise, *J. Appl. Phys.* **83**, 4049 (1998).

<sup>9</sup>K. P. Lieb, in *Encyclopedia on Nanoscience and Nanotechnology*, edited by H. S. Nalwa (American Scientific Publishers, Stevenson Ranch, CA, 2004), Vol. 3, p. 233.

<sup>10</sup>S. Dhar, W. Bolse, and K. P. Lieb, *J. Appl. Phys.* **85**, 3120 (1999).

<sup>11</sup>F. Roccaforte, W. Bolse, and K. P. Lieb, *Appl. Phys. Lett.* **73**, 1349 (1998); *J. Appl. Phys.* **89**, 3611 (2001).

<sup>12</sup>S. Dhar, S. Gasiorek, P. K. Sahoo, U. Vetter, H. Hofsäss, V. N. Kulkarni, and K. P. Lieb, *Appl. Phys. Lett.* (submitted).

<sup>13</sup>M. A. Steven Kalceff and M. R. Phillips, *Phys. Rev. B* **52**, 3122 (1995).

<sup>14</sup>M. A. Steven Kalceff, *Phys. Rev. B* **57**, 5674 (1998).

<sup>15</sup>H. Koyama, *J. Appl. Phys.* **51**, 2228 (1980).

<sup>16</sup>P. K. Sahoo, S. Dhar, S. Gasiorek, and K. P. Lieb, *Nucl. Instrum. Methods Phys. Res. B* **216**, 324 (2004).

<sup>17</sup>J. F. Ziegler and J. P. Biersack, *Computer Program SRIM 2000*.

<sup>18</sup>M. Uhrmacher, K. Pampus, F. J. Bergmeister, D. Purschke, and K. P. Lieb, *Nucl. Instrum. Methods Phys. Res. B* **9**, 234 (1985).

<sup>19</sup>L. R. Doolittle, *Nucl. Instrum. Methods Phys. Res. B* **9**, 344 (1985).

<sup>20</sup>J. Conrad, doctoral thesis, Göttingen (unpublished).

<sup>21</sup>N. D. Skelland and P. D. Townsend, *J. Phys. D* **27**, 1472 (1994); L. Skuja, B. Güttler, D. Schiel and A. R. Silin, *Phys. Rev. B* **58**, 14296 (1998).

<sup>22</sup>H. -J. Fitting, T. Barfels, A. N. Trukhin, and B. Schmidt, *J. Non-Cryst. Solids* **279**, 51 (2001).

<sup>23</sup>H. -J. Fitting, T. Barfels, A. N. Trukhin, B. Schmidt, A. Gulans, and A. von Czarnowski, *J. Non-Cryst. Solids* **303**, 218 (2002).

<sup>24</sup>M. Klimenkov, J. von Borany, W. Matz, R. Grötzschel, and F. Herrmann, *J. Appl. Phys.* **91**, 10062 (2002).

<sup>25</sup>M. Yoshikawa, K. Matsuda, Y. Yamaguchi, T. Matsunobe, Y. Nagasawa, H. Fujino, and T. Yamane, *J. Appl. Phys.* **92**, 7153 (2002).

<sup>26</sup>L. Skuja, *J. Non-Cryst. Solids* **239**, 16 (1998).

<sup>27</sup>T. Shimizu-Iwayama, K. Fujita, S. Nakato, K. Saitoh, T. Fujita, and N. Itoh, *J. Appl. Phys.* **75**, 7779 (1994).

<sup>28</sup>W. Skorupa, R. A. Yankov, I. E. Tyschenko, H. Fröb, T. Böhme, and K. Leo, *Appl. Phys. Lett.* **68**, 2410 (1996).

<sup>29</sup>H. B. Kim, K. H. Chae, C. N. Whang, Y. J. Jeong, M. S. Oh, S. Im, and J. H. Song, *J. Lumin.* **80**, 281 (1999).

<sup>30</sup>L. Rebohle, J. von Borany, W. Skorupa, I. E. Tyschenko, and H. Fröb, *J. Lumin.* **80**, 275 (1999).

<sup>31</sup>L. Rebohle, J. von Borany, R. A. Yankov, W. Skorupa, I. E. Tyschenko, H. Fröb, and K. Leo, *Appl. Phys. Lett.* **71**, 2809 (1997).

<sup>32</sup>L. N. Skuja, A. N. Trukhin and A. Plaudis, *Phys. Status Solidi A* **84**, K153 (1984).

<sup>33</sup>J. M. J. Lopes, F. C. Zawislak, M. Behar, P. F. P. Fichtner, L. Rebohle, and W. Skorupa, *J. Appl. Phys.* **94**, 6059 (2003).

<sup>34</sup>F. Meinardi and A. Paleari, *Phys. Rev. B* **58**, 3511 (1998).

<sup>35</sup>S. Gasiorek, doctoral thesis, Göttingen (unpublished).